HHS Public Access

Author manuscript

Am J Sports Med. Author manuscript; available in PMC 2021 December 01.

Published in final edited form as:

Am J Sports Med. 2020 December ; 48(14): 3503–3514. doi:10.1177/0363546520966721.

ACL Graft Tunnel Placement and Graft Angle are Primary Determinants of Internal Knee Mechanics following Reconstructive Surgery

Michael F. Vignos, PhD,
Department of Mechanical Engineering, University of Wisconsin – Madison 1513 University Avenue, Madison, WI, USA 53706

Colin R. Smith, PhD,
Department of Mechanical Engineering, University of Wisconsin – Madison 1513 University Avenue, Madison, WI, USA 53706

Joshua D. Roth, PhD,
Department of Mechanical Engineering, University of Wisconsin – Madison1513 University Avenue, Madison, WI, USA 53706

Jarred M. Kaiser, PhD,
Department of Mechanical Engineering, University of Wisconsin – Madison 1513 University Avenue, Madison, WI, USA 53706

Geoffrey S. Baer, MD, PhD Final Degree(s): MD, PhD,
Department of Orthopedics and Rehabilitation, University of Wisconsin - Madison, 1685 Highland Avenue, Madison, WI, USA 53705

Richard Kijowski, MD,
Department of Radiology, University of Wisconsin - Madison, 600 Highland Avenue, Madison, WI 53792

Darryl G. Thelen, PhD
Department of Mechanical Engineering, University of Wisconsin – Madison 1513 University Avenue, Madison, WI, USA 53706

Abstract

Background: Graft placement is a modifiable and often discussed surgical factor in ACL reconstruction (ACLR). However, the sensitivity of functional knee mechanics to variability in graft placement is not well understood.

Purpose: (1) Investigate the relationship between ACL graft tunnel location, graft angle, and tibiofemoral kinematics in ACLR patients

(2) Compare experimentally measured relationships to those observed with a computational model to assess the predictive capabilities of the model

mvignos@wisc.edu .

(3) Use the computational model to determine the effect of varying ACL graft tunnel placement on tibiofemoral joint mechanics during walking

Study Design: Controlled Laboratory Study

Methods: Eighteen subjects that had previously undergone an ACLR were tested. Bilateral ACL footprint location and graft angle were assessed using magnetic resonance images (MRI). Bilateral knee laxity was assessed at the completion of rehabilitation. Dynamic MRI was used to measure tibiofemoral kinematics and cartilage contact during active movement. Five-hundred virtual ACLR models were created from a nominal computational knee model by varying ACL footprint locations, graft stiffness, and initial tension. Laxity tests, active knee extension, and walking were simulated with each virtual ACLR model. Correlations between internal knee mechanics and ACL graft tunnel location and angle were determined for both the ACLR patients and the virtual ACLR models.

Results: Static and dynamic MR imaging revealed that a more vertical graft in the sagittal plane was correlated ($P<0.05$) with a greater laxity compliance index and greater anterior tibial translation and internal tibial rotation during active knee extension. Similarly, knee extension simulations with the virtual ACLR models revealed that a more vertical graft led to greater laxity compliance index, anterior translation, and internal rotation. These effects extended to simulations of walking, with a more vertical ACL graft inducing greater anterior tibial translation, ACL loading, and posterior migration of contact on the tibial plateaus.

Conclusions: This study provides clinical evidence from ACLR patients and complementary modeling that functional post-operative knee mechanics are sensitive to graft tunnel locations and graft angle. Of the factors studied, the sagittal angle of the ACL was particularly influential on knee mechanics.

Clinical Relevance: Early onset osteoarthritis (OA) from altered cartilage loading following ACLR is common. This study shows that post-operative cartilage loading is sensitive to graft angle; therefore, variability in graft tunnel placement resulting in small deviations from the anatomic ACL angle might contribute to the elevated risk of OA following ACLR.

Keywords

biomechanics; ACL reconstruction; osteoarthritis; anatomic graft placement

1. Introduction

The placement of anterior cruciate ligament (ACL) graft tunnels is an important surgical factor in ACL reconstruction (ACLR) procedures. Tunnel placement determines the femoral and tibial graft footprints and is a primary determinant of graft angle in the frontal and sagittal planes. Many current ACLR techniques aim to position the graft within the native ACL footprints with the goal of restoring normal knee laxity.[16,39,45,68] However, in practice, variability in arthroscopic techniques results in ACL graft footprints that often deviate from the native footprints.[2,49,57] It is important to understand the effects of such surgical variability on knee behavior because abnormal joint loading likely contributes to the initiation and progression of cartilage damage patterns characteristic of osteoarthritis.[4,10,21,28]

Dynamic imaging technologies have identified systematic abnormalities in kinematics and cartilage contact patterns in ACLR patients. For example, prior studies detected a bias toward external tibial rotation during active movement,[30,35,63] which results in a posterior shift of contact on the medial tibial plateau.[31] There is some evidence that graft angle contributes to these asymmetries in ACLR knee mechanics, with a more vertical graft in the sagittal plane associated with greater side-to-side differences in anterior tibial translation and internal tibial rotation.[1,51,53] However, a major challenge in ACLR patient imaging studies is decoupling the effect of ACL graft tunnel location and graft angle from other surgical factors, such as graft type,[65] stiffness,[48,62] sand initial tension,[14,46] which also influence internal knee loading.

To complement ACLR patient studies, computational models can be used to decouple the influence of multiple surgical factors on internal joint mechanics.[7,8,25,43] For example, Dhaher et al.[25] used a finite element model to simulate an ACL reconstructive procedure using a bone—patellar-tendon—bone autograft. That study found that anterior joint laxity measured during an anterior drawer test is primarily dependent on tunnel placement and secondarily on graft initial tension. Other modeling studies have investigated the effects of ACL femoral footprint location, stiffness, and initial tension on joint laxity.[7,43] However, these previous studies did not provide any validation of the model predictions. It also remains unclear how laxity measures relate to knee behavior during functional tasks such as walking.

The objectives of this study were (1) to investigate the relationship between ACL graft tunnel location, graft angle in the frontal and sagittal planes, and tibiofemoral kinematics in ACLR patients, (2) to compare these experimentally measured relationships to those observed with a computational model to assess the predictive capabilities of the model, and (3) to use the computational model to determine the effect of varying ACL graft tunnel placement on tibiofemoral joint mechanics during walking. Based on these objectives, we hypothesized that (1) a more vertical graft in the sagittal plane would correlate with greater joint laxity, anterior tibial translation, and internal tibial rotation in ACLR patients, (2) a similar relationship between ACL graft tunnel location, graft angles, and tibiofemoral kinematics would be observed between experiments and simulations, and (3) a more vertical graft in the sagittal plane would lead to altered tibiofemoral kinematics, cartilage contact patterns, and ACL loading during simulated walking.

2. Methods

Participants

Potential subjects were identified from the University of Wisconsin Health Sports Medicine Outcomes Program database. Eligible subjects were patients who underwent a primary, unilateral ACLR within the past one to four years, had no other concurrent ligament damage, had no post-operative complications, and had no history of pain, injury, surgery, or inflammatory or crystalline-induced arthritis in the contralateral knee. Based on previous work investigating the relationship between ACL angle and tibiofemoral kinematics during walking,[53] it was determined that a minimum of 14 subjects would need to be tested in order to achieve a significant coefficient of determination with a power of 80% and α =

0.05.[26] Eighteen subjects agreed to participate in the study (nine male, nine female; 24.8 ± 5.7 [mean ± standard deviation] years; 78.9 ± 16.5 kg; 20.2 ± 8.7 months post-surgery). The graft type used for the ACLR (nine bone—patellar-tendon—bone grafts, nine hamstrings tendon grafts) and the presence of absence of meniscus tears (one subject with small stable medial and lateral meniscal tears, two subjects with small partial lateral meniscectomies) were not controlled. Subjects provided written informed consent according to the University of Wisconsin-Madison Institutional Review Board-approved protocol.

Clinical Assessment of Knee Anterior Laxity

Licensed physical therapists at the UW Health Sports Medicine Clinic assessed anterior laxity in reconstructed and contralateral knees following each subject's clearance from post-surgical rehabilitation (9.2 ± 3.5 months post-op). Anterior tibial translation was measured with a KT-1000 arthrometer under 67 N (15 lbs) and 89 N (20 lbs) of anterior load (Figure 1). The compliance index was computed as the difference in anterior tibial translation under these two loads.[3]

Magnetic Resonance Imaging

Each subject underwent a static bilateral magnetic resonance imaging (MRI) protocol using an 8-channel phased array extremity coil (InVivo, Orlando, FL) within a 3.0 T clinical MR scanner (Discovery MR750, GE Healthcare, Waukesha, WI). A three-dimensional (3D) spoiled gradient recall-echo with iterative least squares estimation of fat-water separation (IDEAL-SPGR) sequence (in-plane resolution = 0.37 × 0.37 mm; slice thickness = 0.9 mm) was used to obtain high-resolution images of the knee to characterize bone geometry. The IDEAL-SPGR images were manually segmented (MIMICS, Materialise Group, Leuven, Belgium) to create 3D models of the femoral and tibial bone geometries (Figure 1). A 3D fast spin-echo (FSE) Cube sequence (in-plane resolution = 0.39 × 0.39 mm; slice thickness = 1.0 mm) was used to characterize ACL graft footprint locations and graft angle. The 3D FSE Cube images were manually segmented to create models of the contralateral native ACL and ACL graft geometries. All models were smoothed and converted into triangular meshes (Geomagic Studio, 3D Systems, Rock Hill, SC and MeshLab, Visual Computing Lab-ISTI-CNR, Pisa, Italy). Anatomic coordinate systems were independently defined for the femoral and tibial bone models.[44]

The native ACL and ACL graft footprints were identified as the intersections of the ACL meshes with the femoral and tibial bone meshes. The ACL footprint locations were defined as the centroid of the femoral and tibial footprints (Figure 1). The ACL angle was determined by fitting a cylinder to the mid-substance of the ACL and then finding the angle between that cylinder and the tibial plateau in both the frontal and sagittal planes. The ACL angle was computed with the knee in the MRI scanning posture (approximately 10° knee flexion).

Dynamic MRI was performed bilaterally to characterize tibiofemoral kinematics during active movement. Subjects were positioned supine in the scanner with their lower leg secured to an inertial loading device[66] (Figure 1). Cyclic knee flexion-extension was voluntarily performed at 0.5 Hz, with the device inducing active quadriceps loading with

knee flexion.[66,67] Volumetric MRI data was continuously acquired for five minutes using a vastly under-sampled isotropic projections spoiled gradient-echo (VIPR-SPGR) sequence (1.5-mm isotropic resolution; repetition time, 4 ms; echo time, 1.4 ms; flip angle, 8°; field of view, 48 cm). Image data across cycles were sorted into similar phases of the flexion-extension cycle using knee angle as measured via an MRI-compatible rotary encoder attached to the lever arm (Micronor Inc., Camarillo, CA). The sorted data were reconstructed into 60 volumetric image sets throughout the flexion-extension cycle.[33] Dynamic MRI was performed bilaterally to characterize tibiofemoral kinematics during active movement. Subjects were positioned supine in the scanner with their lower leg secured to an inertial loading device[66] (Figure 1). Cyclic knee flexion-extension was voluntarily performed at 0.5 Hz, with the device inducing active quadriceps loading with knee flexion.[66,67] Volumetric MR data was continuously acquired for five minutes using a SPGR sequence with vastly under-sampled isotropic projections (SPGR-VIPR; 1.5-mm isotropic resolution; repetition time, 4 ms; echo time, 1.4 ms; flip angle, 8°; field of view, 48 cm). Image data across cycles were sorted into similar phases of the flexion-extension cycle using knee angle as measured via an MRI-compatible rotary encoder attached to the lever arm (Micronor Inc., Camarillo, CA). The sorted data were reconstructed into 60 volumetric image sets throughout the flexion-extension cycle.[33]

Tibiofemoral kinematics were measured by registering the femoral and tibial geometries to the dynamic MRIs at each frame of the motion cycle.[33,34] Tibiofemoral translations were defined as the 3D position of the tibia relative to the femur. Tibiofemoral orientation was defined by successive flexion, adduction, and internal rotation angles of the tibia relative to the femur.[29] Tibiofemoral kinematics were low-pass filtered with a cut-off frequency of 5 Hz. Kinematics metrics were defined as the tibiofemoral translations and rotations at peak knee flexion. While peak knee flexion varied across subjects (range = 35° to 48°), this instance was chosen because it corresponds closely to peak quadriceps loading.[66] Tibiofemoral kinematics were measured by registering the femoral and tibial geometries to the dynamic MRIs at each frame of the motion cycle.[33,34] Tibiofemoral translations were defined as the three-dimensional position of the tibia relative to the femur. Tibiofemoral orientation was defined by successive flexion, adduction, and internal rotation angles of the tibia relative to the femur.[29] Tibiofemoral kinematics were low-pass filtered with a cut-off frequency of 5 Hz. This method of assessing tibiofemoral kinematics using dynamic MRI has been shown to have a bias of less than 0.8° and 0.5 mm and a precision of less than 0.9° and 0.5 mm.[34] Kinematics metrics were defined as the tibiofemoral translations and rotations at peak knee flexion. While peak knee flexion varied across subjects (range = 35° to 48°), this instance was chosen because it corresponds closely to peak quadriceps loading.[66]

Virtual ACL Reconstructions

A computational knee model was used to simulate ACL reconstructions (Figure 1). The knee model was previously constructed from high-resolution MRIs of a healthy adult knee.[37] The model includes representations of the femur, patella, tibia, and medial and lateral menisci. An elastic foundation formulation was used to compute cartilage-cartilage and cartilage-meniscal contact pressures.[9,59] Fourteen major knee ligaments and seven

meniscal attachments were represented as bundles of ligament strands with their origins and insertions determined from the MRIs. Ligament strands were defined as nonlinear springs characterized by their stiffness and slack length. Stiffness parameters for individual ligaments were computed as the product of the ligament cross-sectional areas, as measured from MRIs, and an assumed elastic modulus of 125 MPa.[20] Slack lengths were adapted from previous studies.[55,56]

The knee model was incorporated into an existing lower-limb model with 44 muscles acting about the hip, knee, and ankle joints.[5] The combined model was implemented in the Software for Interactive Musculoskeletal Modeling (SIMM). The Dynamics Pipeline (Musculographics, Inc., Santa Rosa, CA) and SD/Fast (Parametric Technology Corp., Needham, MA) were used to generate the multibody dynamics equations of motion.[24] The model was previously validated by comparing simulated knee mechanics to measured tibiofemoral and patellofemoral kinematics.[37] This validated model will subsequently be referred to as the native model.

A total of 500 virtual ACLR models were created from the native model. Each virtual ACLR model was generated by simultaneously varying the ACL footprint locations, stiffness, and initial tension within bounds representative of those observed clinically.[17,41,64] Femoral footprints were randomly varied within ±5 mm of the native location in the anterior-posterior (A-P) and superior-inferior (S-I) directions. Tibial footprints were randomly varied within ±5 mm of the native location in the A-P and medial-lateral (M-L) directions. This range was selected to approximate the variability observed in the ACLR patients in the present study. For each virtual ACLR model, the ACL footprints were not projected back onto the bone surface after moving the footprint location. This approach was used to avoid inducing M-L variations in the femoral footprint and S-I variations in the tibial footprint, which could have led to confounding effects on knee mechanics. This resulted in minimal residual distance between the ACL footprint and the bone surface for some of the virtual ACLR models, with a maximum residual distance of approximately 2 mm between the femoral footprint and the bone surface. ACL stiffness was randomly varied between 150 N/mm and 750 N/mm, with this range defined based on the stiffness in the native model ± 50%.[58] ACL initial tension at full knee extension was randomly varied between 0 N and 150 N.[41,64] This was performed by setting a parameter within the force-length relationship of the ACL that corresponded to the ACL initial tension at full knee extension.[12]

Simulated Movements

Each of the 500 virtual ACLR models and the native model were used in simulations of a KT-1000 laxity assessment, active knee extension, and over-ground walking. The simulation of the KT-1000 assessment consisted of a forward dynamic simulation with the knee flexion angle fixed at 20° and a point load applied to the tibia in the anterior direction (Figure 1). The load was applied 20 cm distal to the tibiofemoral joint line and was ramped from 0 N to 89 N to replicate the clinical assessment. The anterior translation of the tibia relative to the femur under applied loads of 67 N and 89 N was extracted. These anterior translations were used to compute the compliance index of the virtual ACLR models and the native model.

Active knee extension was simulated with the knee flexion angle fixed at 30°, and the quadriceps and hamstrings muscles activated to 15% and 5%, respectively (Figure 1). The 30° angle reflected the average peak knee flexion reached by ACLR patients during the dynamic MRI task. The muscle activations were equivalent to those observed at the time of peak ACL loading during simulated gait from the final portion of this study. These activations resulted in combined quadriceps and hamstrings muscle forces of 655 N and 130 N, respectively. At the end of each simulation, the tibiofemoral kinematics that resulted from the applied muscle loads were extracted.

Finally, the knee behavior during over-ground walking for each of the virtual ACLR models was simulated. Whole body kinematics and ground reaction forces were previously measured for the subject from which the knee model was generated.[37] The Concurrent Optimization of Muscle Activations and Kinematics (COMAK) simulation routine was used to calculate the muscle forces and internal knee mechanics at each frame across the gait cycle.[15,60] The weighted sum of squared muscle activations was minimized to resolve muscle redundancy.[15] The relationship between graft tunnel locations, graft angle, and simulated tibiofemoral kinematics, contact pressure on the medial and lateral tibial plateaus, and the peak ACL loading was examined.

Statistical Analysis

Non-anatomic ACL graft tunnel locations and graft angle were assessed experimentally by computing side-to-side differences (reconstructed minus contralateral) in the ACL femoral and tibial footprint locations and the ACL angle in the frontal and sagittal planes for the ACLR patients. Paired t-tests ($\alpha = 0.05$) were performed to determine if significant biases existed in the side-to-side differences in graft tunnel location and graft angle.

Asymmetric knee mechanics were assessed by computing side-to-side differences (reconstructed minus contralateral) in the anterior laxity and tibiofemoral kinematics metrics. A least-squares linear regression was performed between the non-anatomic ACL graft tunnel location and graft angle metrics and the asymmetric knee mechanics metrics ($\alpha = 0.05$). The slope of the linear regression model (β) was used to assess the sensitivity of post-operative knee mechanics to these surgical factors.

Non-anatomic ACL graft tunnel locations, graft angle, stiffness, and initial tension were assessed by computing differences in these metrics between each of the 500 virtual ACLR models and the native knee model (virtual ACLR model minus native). Similarly, abnormal knee mechanics were assessed by computing differences between the ACLR simulations and the native simulations. This was done for all simulations (i.e. the KT-1000, knee extension task, and gait simulations). A least-squares linear regression was performed between the abnormal knee mechanics metrics and the non-anatomic ACL graft tunnel locations, graft angle, stiffness, and initial tension metrics to assess the effect of varying these surgical factors on post-operative knee mechanics. The slope of the linear regression model (β) was used to assess the sensitivity of knee mechanics to these surgical factors. To validate the simulations, the predicted relationship between graft tunnel locations and graft angle on knee mechanics from the KT-1000 and active knee extension simulations were

compared to those observed from the experimental KT-1000 assessment and active knee flexion-extension results, respectively (Figure 1).

Results

In Vivo ACLR Study

Side-to-side differences in ACL geometry measured in the ACLR patients (ACL graft minus native ACL) were −2.3 ± 0.8 mm (range: −6.8 to 2.3 mm) in the A-P direction and 0.2 ± 0.3 mm (range: −3.6 mm to 4.9 mm) in the M-L direction for the tibial tunnel location, 0.7 ± 0.6 mm (range: −4.2 mm to 6.4 mm) in the A-P direction and −0.5 ± 2.7 mm (range: −8.8 mm to 10.3 mm) in the S-I direction for the femoral tunnel location, and 0.7 ± 0.01° (range: −11.5° to 13.5°) in the frontal and −2.6 ± 1.4° (range: −18.4° to 8.1°) in the sagittal plane. A significant difference was only observed in the tibial tunnel A-P location ($p = 0.001$).

Non-anatomic ACL graft angle was significantly related to side-to-side differences in anterior knee laxity and tibiofemoral kinematics in the ACLR patients (Table 1). Specifically, a more vertical graft in the sagittal plane was related to a greater compliance index during KT-1000 assessment of anterior laxity (Figure 2, $P = 0.049$). However, there were no significant correlations between ACL graft angle and absolute anterior tibial translation during KT-1000 assessment. During active knee flexion-extension, a more vertical graft in the sagittal plane was also linked to greater anterior tibial translation ($P = 0.049$), internal tibial rotation ($P = 0.042$), and tibial adduction angle ($P = 0.013$, $\beta = 0.15$ $^{deg}/_{deg}$) at peak knee flexion during dynamic MRI measurements (Figure 2). Additionally, a more vertical graft in the frontal plane and a more superior femoral footprint location were significantly related to greater medial tibial translation measured using dynamic MRI ($P = 0.046$, $\beta = 0.089$ $^{mm}/_{deg}$ and $P = 0.021$, $\beta = 0.26$ $^{mm}/_{mm}$, respectively).

Computational Model Study

Simulated variations in the femoral tunnel location of +/− 5 mm in the AP and SI directions and the tibial tunnel location of +/− 5 mm in the AP and ML directions led to a range in the ACL sagittal plane angle of 33.8° to 79.3° and in the ACL frontal plane angle of 56.5° to 85.6° (Figure 3). These virtual ACLR simulations predicted causal relationships between ACL graft tunnel locations and graft angle and knee mechanics that were consistent with trends observed in the ACLR patients (Table 1). For example, during the simulated KT-1000 assessment, the sagittal plane angle of the ACL was positively correlated with the compliance index (Figure 2, $\beta = 0.0083$ $^{mm}/_{deg}$). Similarly, a more vertical graft in the sagittal plane was correlated with increased anterior tibial translation ($\beta = 0.12$ $^{mm}/_{deg}$), internal tibial rotation ($\beta = 0.074$ $^{deg}/_{deg}$), and tibial adduction ($\beta = 0.031$ $^{deg}/_{deg}$) during simulated knee extension. Finally, a more vertical graft in the frontal plane and a more superior femoral footprint position led to greater medial tibial translation ($\beta = 0.041$ $^{mm}/_{deg}$ and $\beta = 0.010$ $^{mm}/_{mm}$, respectively).

The ACLR simulations also provided insights into the sensitivity of knee mechanics during walking to ACL graft tunnel locations, graft angle, stiffness, and initial tension (Figure 4, Table S1). At the time of peak ACL load, the model predicted that a more vertical graft in

the sagittal plane and a more posterior tibial footprint location resulted in increased anterior tibial translation. In addition, a more vertical graft in the sagittal plane and a more anterior femoral footprint location increased peak ACL load. A greater ACL graft initial tension and stiffness led to a decrease in the anterior translations (R^2 = 0.48, β = −0.02 $^{mm}/_{N}$ and R^2 = 0.089, β = −0.003 $^{mm}/_{N/mm}$, respectively) and an increase in ACL force (R^2 = 0.59, β = 0.80 $^{N}/_{N}$ and R^2 = 0.19, β = 0.12 $^{N}/_{N/mm}$, respectively) at the time of peak ACL load (Figure S1).

These effects of ACL graft tunnel location, graft angle, stiffness, and initial tension on kinematics during walking extended to cartilage contact (Figure 5, Table S1). During the stance phase, a more vertical graft in the sagittal plane led to a posterior migration of the center of pressure and an increase in the maximum contact pressure on the medial tibial plateau (Figure 6; R^2 = 0.23, β = −0.049 $^{mm}/_{deg}$ and R^2 = 0.28, β = 0.023 $^{MPa}/_{deg}$, respectively) and lateral tibial plateau (R^2 = 0.20, β = −0.037 $^{mm}/_{deg}$ and R^2 = 0.23, β = 0.0036 $^{MPa}/_{deg}$, respectively). Additionally, a more posterior tibial footprint led to a posterior migration of the center of pressure on the medial tibial plateau (R^2 = 0.27, β = 0.16 $^{mm}/_{mm}$) and lateral tibial plateau (R^2 = 0.30, β = 0.14 $^{mm}/_{mm}$), an increase in contact pressure on the medial plateau (R^2 = 0.25, β = −0.066 $^{MPa}/_{mm}$), and a decrease in contact pressure on the lateral plateau (R^2 = 0.28, β = 0.012 $^{MPa}/_{mm}$). A reduction in the graft initial tension and stiffness led to a posterior migration of the center of pressure on the medial plateau (Figure S2; R^2 = 0.50, β = 0.02 $^{mm}/_{N}$ and R^2 = 0.083, β = 0.0021 $^{mm}/_{N/mm}$, respectively) and lateral plateau (R^2 = 0.47, β = 0.016 $^{mm}/_{N}$ and R^2 = 0.10, β = 0.0018 $^{mm}/_{N/mm}$, respectively). Decreasing the graft initial tension and stiffness also led to an increase in maximum contact pressure on the medial plateau (R^2 = 0.40, β = −0.0075 $^{MPa}/_{N}$ and R^2 = 0.056, β = 0.0007 $^{MPa}/_{N/mm}$, respectively) and a decrease in maximum contact pressure on the lateral plateau (R^2 = 0.56, β = 0.0048 $^{MPa}/_{N}$ and R^2 = 0.23, β = 0.00079 $^{MPa}/_{N/mm}$, respectively).

Discussion

This study of ACLR patients and virtual ACLR models investigated the influence of surgical factors on knee mechanics. Our results demonstrate that the placement of the graft in the sagittal plane is a primary geometric determinant of internal knee mechanics. A more vertical graft placement induced greater laxity, anterior tibial translation, peak graft force, and elevated cartilage contact pressure on the posterior aspect of the tibial plateau during walking. ACL graft placement effects were significant even when simultaneously varying graft stiffness and initial tension to capture patient-to-patient differences, suggesting that graft angle is a primary surgical factor affecting long-term joint biomechanics. To our knowledge, this is the first study to integrate measurements on ACLR patients and biomechanical models to isolate the effect of multiple ACLR surgical factors on post-operative knee mechanics. These findings provide insight into the relative contributions of ACL graft tunnel placement and graft angle on long-term patient outcomes following ACLR.

Optimal ACL graft placement has long been debated, with the target for ACL graft tunnel location varying over time. Contemporary approaches have trended towards the goal of restoring the native ACL footprints (i.e. an anatomic graft placement).[18,52] This technique is supported by prior studies that have detected links between non-anatomic graft angle and abnormal knee mechanics. For example, a more vertical graft in the sagittal plane has been

linked with greater anterior and rotational laxity[16,39] and larger anterior tibial translation, medial tibial translation, and internal rotation in ACLR patients during a quasi-static lunge.[1] We observed similar results in the ACLR patients in this study, with a non-anatomic sagittal graft angle correlated with side-to-side differences in anterior laxity measures, and both anterior tibial translation and internal tibial rotation during active movement. The causality of these relationships was confirmed with a computational model, which predicted similar relationships between graft tunnel locations, graft angle, laxity, and tibiofemoral kinematics to those measured in ACLR patients.

Previous ACLR techniques aimed to place the femoral tunnel anterior of the native ACL footprint (i.e. a non-anatomic ACLR) with the goal of achieving a graft that remained isometric throughout the knee range of motion.[50] One of the motivators of this approach was to minimize loading on the ACL graft and, thus, reduce the risk of graft rupture. Previous cadaveric studies provided support to this approach by showing that this technique can achieve a relatively isometric ACL during passive knee flexion-extension, typically using a transtibial, one-incision drilling technique.[40,47,69] However, it has also been observed that this surgical technique commonly results in a more vertical graft in the sagittal plane and is associated with an increased risk of secondary ACL rupture.[32,42] The findings of this study provide a mechanistic understanding of the pitfalls of this previous approach by showing that a more vertical graft in the sagittal plane and a more anterior femoral tunnel location leads to increased force in the ACL during gait. However, the results of this study also indicate that targeting a more horizontal ACL graft, with the goal of reducing ACL force, is not optimal due to potential changes in cartilage loading. Thus, these findings provide additional support for targeting the native ACL footprint location and angle when performing ACLR.

The consistency between the results from ACLR patients and virtual ACLR models provided confidence in extending the model to investigate the influence of surgical factors on more functional knee mechanics. We investigated over-ground walking because altered cartilage loading patterns during locomotion are considered to be one of the primary factors in initiating cartilage damage in ACLR knees.[21] These simulations again revealed a strong link between sagittal plane graft angle and functional knee mechanics, with a more vertical graft leading to greater anterior tibial translation, ACL loading, and cartilage contact pressure (Figure 6). Both ACL stiffness and initial ACL tension also affected the anterior tibial translation and cartilage loading seen in walking though there is the potential for stiffness and tension to adapt over time.[6,11,13] These findings suggest that surgical variability in graft tunnel locations, graft angle, stiffness, and initial tension all contribute to short-term knee behavior following ACLR, with graft angle being the surgical factor that has a consistent effect in the long-term.

The sensitivities of internal knee mechanics to variations in ACL graft tunnel locations and graft angle observed in this study may help in restoring common abnormalities seen in ACLR patients. Many studies have reported a bias towards external tibial rotation in ACLR knees during a range of tasks.[27,30,35,54,63] Further, a prior study using biplane fluoroscopy during a quasi-static lunge found that ACLR knees exhibited a posterior-lateral shift in cartilage contact location on the tibial plateaus.[31] Our study suggests these altered

kinematics and cartilage contact patterns could arise from non-anatomic ACL graft tunnel placements. In particular, we found that the angle of the graft in the sagittal plane was linked to asymmetries in external tibial rotation (Table 1) and anterior-posterior cartilage contact location (Figure 4). In our surgical simulations, the sagittal plane graft angle was primarily influenced by the anterior and superior placement of the femoral footprint and the anterior placement of the tibial footprint (Figure 2). These findings demonstrate the importance of placing the femoral and tibial graft footprint within the anatomic locations to restore normative knee mechanics.

Recent modifications to ACLR surgical techniques have focused on improving the accuracy of graft tunnel placement, thus allowing surgeons to more closely re-create anatomic femoral and tibial graft footprints. Traditional transtibial graft placement typically results in femoral footprints an average of 8 to 9 mm from the center of the native femoral footprint.[2,36] The use of two-incision arthroscopic techniques, which place the femoral and tibial tunnels independently, has led to increased accuracy in tunnel placement relative to the native footprint locations,[52] with an average error of 3 mm in the femoral footprint location.[2] However, our findings suggest that errors in tunnel placement of that magnitude can induce substantial changes in ACL orientation (Figure 3), and thereby contribute to residual abnormal knee mechanics. Thus, further advancements in surgical technique, such as highly accurate placement of both femoral and tibial tunnels using computer-assisted and robotic guidance,[19,49] may be important to fully restore ACL orientation and normative mechanics.

Four limitations should be considered when interpreting the findings of the present study. First, we did not control for graft type[65] or initial graft tension[14,46] in ACLR patient cohort. To account for these factors that vary from patient to patient, we randomly varied graft stiffness and initial tension, in addition to graft tunnel placement, in the virtual ACLR models. Initial tension had a larger effect on simulated knee mechanics than graft stiffness. However, it has previously been shown that graft stiffness and tension change following surgery due to graft relaxation and remodeling.[6,11,13] Hence, of the parameters considered, graft tunnel placement is the factor that is most controllable by surgeons over the long-term. Second, the simulation technique used in this study was unable to account for the differences in morphology that exist between a native ACL and an ACL graft, given that the ACL is represented by a bundle of nonlinear spring elements. However, recent developments in coupled finite element and multi-body dynamic models[38] may provide the capability to account for this difference in future work and to determine if differences in graft morphology affect optimal placement. Third, we did not simulate variations in muscle coordination strategies or walking dynamics, which have been shown to vary across ACLR patients[23] and can potentially influence *in vivo* knee behavior.[22] In future work, we plan to extend our study of ACLR surgical parameters to include possible neuromuscular adaptations in walking behavior to gain insights into rehabilitation protocols for ACLR. Finally, we used a single knee model with fixed bone and cartilage geometry as segmented from MRIs. Previous studies have shown a link between variations in bone geometry and tibiofemoral kinematics.[61] Thus, the variability of changes in knee biomechanics determined using our model is likely conservative relative to what would be seen clinically in patients with variable bone and cartilage geometry (Figure 3). However, this does not alter the conclusion from our study that knee laxity, knee kinematics, cartilage contact, and ACL

loading following ACLR are sensitive to surgical variability in ACL graft placement. Future work, with a larger cohort of patients, may allow for an experimental assessment of the relative contributions of bone geometry and ACL graft tunnel placement on knee mechanics following ACLR.

In conclusion, the findings of this study provide evidence that knee laxity, knee kinematics, cartilage contact, and ACL loading following ACLR are sensitive to surgical variability in ACL graft placement. This is important to consider given the links between abnormal knee mechanics, cartilage degeneration, and early onset OA in ACLR knees. Coupling these findings with future investigations to establish a threshold of acceptable altered cartilage loading could provide a better understanding of the accuracy in graft tunnel placement needed to improve long-term outcomes of ACLR.

Supplementary Material

Refer to Web version on PubMed Central for supplementary material.

References

1. Abebe E, Utturkar GM, Taylor DC, et al.The effects of femoral graft placement on in vivo knee kinematics after anterior cruciate ligament reconstruction. J Biomech. 2011;44(5):924–929. doi:10.1016/j.jbiomech.2010.11.028. [PubMed: 21227425]
2. Abebe ES, Moorman CT, Dziedzic TS, et al.Femoral Tunnel Placement During Anterior Cruciate Ligament Reconstruction An In Vivo Imaging Analysis Comparing Transtibial and 2-Incision Tibial Tunnel–Independent Techniques. Am J Sports Med. 2009;37(10):1904–1911. doi:10.1177/0363546509340768. [PubMed: 19687514]
3. Alford JW, Bach BR. Arthrometric Aspects of Anterior Cruciate Ligament Surgery Before and After Reconstruction With Patellar Tendon Grafts. Tech Orthop. 2005;20(4):421–438. doi:10.1097/01.bto.0000190441.56526.92.
4. Anderst WJ, Tashman S. The association between velocity of the center of closest proximity on subchondral bones and osteoarthritis progression. J Orthop Res. 2009;27(1):71–77. doi:10.1002/jor.20702. [PubMed: 18634007]
5. Arnold EM, Ward SR, Lieber RL, Delp SL. A Model of the Lower Limb for Analysis of Human Movement. Natl Inst Heal. 2011;38(2):269–279. doi:10.1007/s10439-009-9852-5.A.
6. Arnold MR, Lie DTT, Verdonschot N, De Graaf R, Amis AA, Van Kampen A. The remains of anterior cruciate ligament graft tension after cyclic knee motion. Am J Sports Med. 2005;33(4):536–542. doi:10.1177/0363546504269938. [PubMed: 15722282]
7. Baldwin MA, Laz PJ, Stowe JQ, Rullkoetter PJ. Efficient probabilistic representation of tibiofemoral soft tissue constraint. Comput Methods Biomech Biomed Engin. 2009;12(6):651–659. doi:10.1080/10255840902822550. [PubMed: 19370459]
8. Barry MJ, Kwon TH, Dhaher YY. Probabilistic musculoskeletal modeling of the knee: A preliminary examination of an ACL-reconstruction. 2010 Annu Int Conf IEEE Eng Med Biol Soc EMBC'10. 2010:5440–5443. doi:10.1109/IEMBS.2010.5626511.
9. Bei Y, Fregly BJ. Multibody dynamic simulation of knee contact mechanics. Med Eng Phys. 2004;26(9 SPEC.ISS.):777–789. doi:10.1016/j.medengphy.2004.07.004. [PubMed: 15564115]
10. Beveridge JE, Heard BJ, Shrive NG, Frank CB. Tibiofemoral centroid velocity correlates more consistently with cartilage damage than does contact path length in two ovine models of stifle injury. J Orthop Res. 2013;31(11):1745–1756. doi:10.1002/jor.22429. [PubMed: 23832294]
11. Beynnon BD, Uh BS, Johnson RJ, Fleming BC, Renstrom PA, Nichols CE. The elongation behavior of the anterior cruciate ligament graft in vivo. A long-term follow-up study. Am J Sports Med. 2001;29(2):161–166. doi:10.1177/03635465010290020801. [PubMed: 11292040]

12. Blankevoort L, Huiskes R. Ligament-Bone Interaction in a Three-Dimensional Model of the Knee. J Biomech Eng. 1991;113(August):263–269. [PubMed: 1921352]
13. Blickenstaff KR, Grana WA, Egle D. Analysis of a Semitendinosus Autograft in a Rabbit Model. Am J Sports Med. 1997;25(4):554–559. [PubMed: 9240991]
14. Brady MF, Bradley MP, Fleming BC, Fadale PD, Hulstyn MJ, Banerjee R. Effects of Initial Graft Tension on the Tibiofemoral Compressive Forces and Joint Position After Anterior Cruciate Ligament Reconstruction. Am J Sports Med. 2007;35(3):395–403. doi:10.1177/0363546506294363. [PubMed: 17218659]
15. Brandon S, Smith CR, Thelen DG. Simulation of Soft Tissue Loading from Observed Movement Dynamics. In: Handbook of Human Motion. ; 2017. doi:10.1007/978-3319-30808-1_172-1.
16. Brophy RH, Pearle AD. Single-Bundle Anterior Cruciate Ligament Reconstruction: A Comparison of Conventional, Central, and Horizontal Single-Bundle Virtual Graft Positions. Am J Sports Med. 2009;37(7):1317–1323. doi:10.1177/0363546509333007. [PubMed: 19329787]
17. Brown CH, Wilson DR, Hecker AT, Ferragamo M. Graft-bone motion and tensile properties of hamstring and patellar tendon anterior cruciate ligament femoral graft fixation under cyclic loading. Arthrosc - J Arthrosc Relat Surg. 2004;20(9):922–935. doi:10.1016/j.arthro.2004.06.032.
18. Budny J, Fox J, Rauh M, Fineberg M. Emerging Trends in Anterior Cruciate Ligament Reconstruction. J Knee Surg. 2017;30:63–69. [PubMed: 27018510]
19. Burkart A, Debski RE, McMahon PJ, et al.Precision of ACL tunnel placement using traditional and robotic techniques. Comput Aided Surg. 2001;6(5):270–278. doi:10.1002/igs.10013. [PubMed: 11892003]
20. Chandrashekar N, Mansouri H, Slauterbeck J, Hashemi J. Sex-based differences in the tensile properties of the human anterior cruciate ligament. J Biomech. 2006;39(16):2943–2950. doi:10.1016/j.jbiomech.2005.10.031. [PubMed: 16387307]
21. Chaudhari AMW, Briant PL, Bevill SL, Koo S, Andriacchi TP. Knee kinematics, cartilage morphology, and osteoarthritis after ACL injury. Med Sci Sports Exerc. 2008;40(2):215–222. doi:10.1249/mss.0b013e31815cbb0e. [PubMed: 18202582]
22. Chmielewski TL, Hurd WJ, Rudolph KS, Axe MJ, Snyder-mackler L. Perturbation Training Improves Knee Kinematics and Reduces Muscle Co-contraction After Complete Unilateral Anterior Cruciate Ligament Rupture. Phys Ther. 2005;85(8):740–754. doi:10.1093/ptj/85.8.740. [PubMed: 16048422]
23. Ciccotti MG, Kerlan RK, Perry J, Pink M. An Electromyographic Analysis of the Knee During Functional Activities: II. The Anterior Cruciate Ligament-deficient and - reconstructed Profiles. Am J Sports Med. 1994;22(5):651–658. doi:10.1177/036354659402200513. [PubMed: 7810789]
24. Delp SL, Loan JP. A Computational Framework For Simulating And Analyzing Human And Animal Movement. Comput Sci Eng. 2000:46–55. doi:10.1109/5992.877394.
25. Dhaher YY, Salehghaffari S, Adouni M. Anterior laxity, graft-tunnel interaction and surgical design variations during anterior cruciate ligament reconstruction: A probabilistic simulation of the surgery. J Biomech. 2016. doi:10.1016/j.jbiomech.2016.07.019.
26. Erdfelder E, FAul F, Buchner A, Lang AG. Statistical power analyses using G*Power 3.1: Tests for correlation and regression analyses. Behav Res Methods. 2009;41(4):1149–1160. doi:10.3758/BRM.41.4.1149. [PubMed: 19897823]
27. Georgoulis AD, Papadonikolakis A, Papageorgiou CD, Mitsou A, Stergiou N. Three-dimensional tibiofemoral kinematics of the anterior cruciate ligament-deficient and reconstructed knee during walking. Am J Sports Med. 2003;31(1):75–79. [PubMed: 12531761]
28. Griffin TM, Guilak F. The Role of Mechanical Loading in the Onset and Progression of Osteoarthritis. Exerc Sport Sci Rev. 2005;33(4):195–200. doi:10.1097/00003677200510000-00008. [PubMed: 16239837]
29. Grood ES, Suntay WJ. A joint coordinate system for the clinical description of three-dimensional motions: application to the knee. J Biomech Eng. 1983;105(2):136–144. doi:10.1115/1.3138397. [PubMed: 6865355]
30. Hofbauer M, Thorhauer ED, Abebe E, Bey M, Tashman S. Altered Tibiofemoral Kinematics in the Affected Knee and Compensatory Changes in the Contralateral Knee

After Anterior Cruciate Ligament Reconstruction. Am J Sports Med. 2014;42(11):2715–2721. doi:10.1177/0363546514549444. [PubMed: 25227945]

31. Hosseini A, Van De Velde S, Gill TJ, Li G. Tibiofemoral Cartilage Contact Biomechanics in Patients after Reconstruction of a Ruptured Anterior Cruciate Ligament. J Orthop Res. 2012;November:1781–1788. doi:10.1002/jor.22122. [PubMed: 22528687]
32. Jaecker V, Zapf T, Naendrup JH, et al.High non-anatomic tunnel position rates in ACL reconstruction failure using both transtibial and anteromedial tunnel drilling techniques. Arch Orthop Trauma Surg. 2017;137(9):1293–1299. doi:10.1007/s00402-017-2738-3. [PubMed: 28721590]
33. Kaiser J, Bradford R, Johnson K, Wieben O, Thelen DG. Measurement of Tibiofemoral Kinematics Using Highly Accelerated 3D Radial Sampling. Magn Reson Med. 2013;69:1310–1316. doi:10.1002/mrm.24362. [PubMed: 22693040]
34. Kaiser J, Monawer A, Chaudhary R, et al.Accuracy of model-based tracking of knee kinematics and cartilage contact measured by dynamic volumetric MRI. Med Eng Phys. 2016;38:1–5. doi:10.1016/j.medengphy.2016.06.016. [PubMed: 26697776]
35. Kaiser JM, Vignos MF, Kijowski R, Baer G, Thelen DG. Effect of Loading on In Vivo Tibiofemoral and Patellofemoral Kinematics of Healthy and ACL-Reconstructed Knees. Am J Sports Med. 2017;45(14):3272–3279. doi:10.1177/0363546517724417. [PubMed: 28903010]
36. Kaseta MK, DeFrate LE, Charnock BL, Sullivan RT, Garrett WE. Reconstruction technique affects femoral tunnel placement in ACL reconstruction. Clin Orthop Relat Res. 2008;466(6):1467–1474. doi:10.1007/s11999-008-0238-z. [PubMed: 18404292]
37. Lenhart RL, Kaiser J, Smith CR, Thelen DG. Prediction and Validation of Load-Dependent Behavior of the Tibiofemoral and Patellofemoral Joints During Movement. Ann Biomed Eng. 2015;43(11):2675–2685. doi:10.1007/s10439-015-1326-3. [PubMed: 25917122]
38. Lloyd JE, Stavness I, Fels S. ArtiSynth : A Fast Interactive Biomechanical Modeling Toolkit Combining Multibody and Finite Element Simulation. In: Payan Y, ed. Soft Tissue Biomechanical Modeling for Computer Assisted Surgery. Studies in Mechanobiology, Tissue Engineering and Biomaterials. 11th ed. Berlin, Heidelberg: Springer; 2012:1–41.
39. Loh JC, Fukuda Y, Tsuda E, Steadman RJ, Fu FH, Woo SLY. Knee stability and graft function following anterior cruciate ligament reconstruction: Comparison between 11 o'clock and 10 o'clock femoral tunnel placement. 2002 Richard O'Connor Award Paper Knee. Arthrosc - J Arthrosc Relat Surg. 2003;19(3):297–304. doi:10.1053/jars.2003.50084.
40. Lubowitz JH. Anatomic ACL reconstruction produces greater graft length change during knee range-of-motion than transtibial technique. Knee Surgery, Sport Traumatol Arthrosc. 2014;22(5):1190–1195. doi:10.1007/s00167-013-2694-6.
41. Mae T, Shino K, Matsumoto N, Hamada M, Yoneda M, Nakata K. Anatomical two-bundle versus Rosenberg's isometric bi-socket ACL reconstruction: A biomechanical comparison in laxity match pretension. Knee Surgery, Sport Traumatol Arthrosc. 2007;15(4):328–334. doi:10.1007/s00167-006-0172-0.
42. Marchant BG, Noyes FR, Barber-Westin SD, Fleckenstein C. Prevalence of nonanatomical graft placement in a series of failed anterior cruciate ligament reconstructions. Am J Sports Med. 2010;38(10):1987–1996. doi:10.1177/0363546510372797. [PubMed: 20702859]
43. Mesfar W, Shirazi-Adl A. Biomechanics of changes in ACL and PCL material properties or prestrains in flexion under muscle force-implications in ligament reconstruction. Comput Methods Biomech Biomed Engin. 2006;9(4):201–209. doi:10.1080/10255840600795959. [PubMed: 17132528]
44. Miranda DL, Rainbow MJ, Leventhal EL, Crisco JJ, Fleming BC. Automatic determination of anatomical coordinate systems for three- dimensional bone models of the isolated human knee. J Biomech. 2010;43(8):1623–1626. doi:10.1016/j.jbiomech.2010.01.036. [PubMed: 20167324]
45. Musahl VVarying Femoral Tunnels Between the Anatomical Footprint and Isometric Positions: Effect on Kinematics of the Anterior Cruciate Ligament-Reconstructed Knee. Am J Sports Med. 2005;33(5):712–718. doi:10.1177/0363546504271747. [PubMed: 15722268]
46. Nicholas SJ, D'Amato MJ, Mullaney MJ, Tyler TF, Kolstad K, McHugh MP. A Prospectively Randomized Double-Blind Study on the Effect of Initial Graft Tension on Knee Stability

After Anterior Cruciate Ligament Reconstruction. Am J Sports Med. 2004;32(8):1–6. doi:10.1177/0363546504265924.

47. O'Meara PM, O'Brien WR, Henning CE. Anterior cruciate ligament reconstruction stability with continuous passive motion. The role of isometric graft placement. Clin Orthop Relat Res. 1992; (277):201—209. http://europepmc.org/abstract/MED/1555343.
48. Peña E, Martínez MA, Calvo B, Palanca D, Doblaré M. A finite element simulation of the effect of graft stiffness and graft tensioning in ACL reconstruction. Clin Biomech. 2005;20(6):636–644. doi:10.1016/j.clinbiomech.2004.07.014.
49. Picard F, DiGioia AM, Moody J, et al.Accuracy in tunnel placement for ACL reconstruction. Comparison of traditional arthroscopic and computer-assisted navigation techniques. Comput Aided Surg. 2001;6(5):279–289. doi:10.1002/igs.10014. [PubMed: 11892004]
50. Rayan F, Nanjayan SK, Quah C, Ramoutar D, Konan S, Haddad FS. Review of evolution of tunnel position in anterior cruciate ligament reconstruction. World J Orthop. 2015;6(2):252–262. doi:10.5312/wjo.v6.i2.252. [PubMed: 25793165]
51. Ristanis S, Stergiou N, Siarava E, Ntoulia A, Mitsionis G, Georgoulis AD. Effect of femoral tunnel placement for reconstruction of the anterior cruciate ligament on tibial rotation. J Bone Jt Surg -Ser A. 2009;91(9):2151–2158. doi:10.2106/JBJS.H.00940.
52. Robin BN, Jani SS, Marvil SC, Reid JB, Schillhammer CK, Lubowitz JH. Advantages and Disadvantages of Transtibial, Anteromedial Portal, and Outside-In Femoral Tunnel Drilling in Single-Bundle Anterior Cruciate Ligament Reconstruction: A Systematic Review. Arthrosc - J Arthrosc Relat Surg. 2015;31(7):1412–1417. doi:10.1016/j.arthro.2015.01.018.
53. Scanlan SF, Andriacchi TP. Interactions Between Graft Placement, Gait Mechanics, and Premature Osteoarthritis Following Anterior Cruciate Ligament Reconstruction. J Exp Clin Med. 2011;3(5):207–212. doi:10.1016/j.jecm.2011.09.004.
54. Scanlan SF, Chaudhari AMW, Dyrby CO, Andriacchi TP. Differences in tibial rotation during walking in ACL reconstructed and healthy contralateral knees. J Biomech. 2010;43(9):1817–1822. doi:10.1016/j.jbiomech.2010.02.010. [PubMed: 20181339]
55. Shelburne KB, Torry MR, Pandy MG. Contributions of Muscles, Ligaments, and the Ground-Reaction Force to Tibiofemoral Joint Loading During Normal Gait. J Orthop Res. 2006:1983–1989. doi:10.1002/jor. [PubMed: 16900540]
56. Shin CS, Chaudhari AM, Andriacchi TP. The influence of deceleration forces on ACL strain during single-leg landing: A simulation study. J Biomech. 2007;40:1145–1152. doi:10.1016/j.jbiomech.2008.10.031. [PubMed: 16797556]
57. Sirleo L, Innocenti M, Innocenti M, Civinini R, Carulli C, Matassi F. Post-operative 3D CT feedback improves accuracy and precision in the learning curve of anatomic ACL femoral tunnel placement. Knee Surgery, Sport Traumatol Arthrosc. 2018;26(2):468–477. doi:10.1007/s00167-017-4614-7.
58. Smith CR, Lenhart RL, Kaiser J, Vignos MF, Thelen DG. Influence of Ligament Properties on Tibiofemoral Mechanics in Walking. Journal of Knee Surgery. 2015.
59. Smith CR, Won Choi K, Negrut D, Thelen DG. Efficient computation of cartilage contact pressures within dynamic simulations of movement. Comput Methods Biomech Biomed Eng Imaging Vis. 2016;1163(March):1–8. doi:10.1080/21681163.2016.1172346.
60. Smith CRCR Vignos MFMF, Lenhart RLRL, Kaiser J, Thelen DGDG. The Influence of Component Alignment and Ligament Properties on Tibiofemoral Contact Forces in Total Knee Replacement. J Biomech Eng. 2016;138(c):1–10. doi:10.1115/1.4032464.
61. Smoger LM, Fitzpatrick CK, Clary CW, et al.Statistical Modeling to Characterize Relationships Between Knee Anatomy and Kinematics. J Orthop Res. 2015;33(11):1620–1630. doi:10.1002/jor.22948. [PubMed: 25991502]
62. Suggs J, Wang C, Li G. The effect of graft stiffness on knee joint biomechanics after ACL reconstruction - A 3D computational simulation. Clin Biomech. 2003;18(1):35–43. doi:10.1016/S0268-0033(02)00137-7.
63. Tashman S, Collon D, Anderson K, Kolowich P, Anderst W. Abnormal Rotational Knee Motion During Running After Anterior Cruciate Ligament Reconstruction. Am J Sports Med. 2004;32(4):975–983. doi:10.1177/0363546503261709. [PubMed: 15150046]

64. Tohyama H, Yasuda K. Significance of graft tension in anterior cruciate ligament reconstruction. Basic background and clinical outcome. Knee Surg Sports Traumatol Arthrosc. 1998;6 Suppl 1:S30–7. doi:10.1007/s001670050220. [PubMed: 9608461]

65. Webster KE, Feller JA. The knee adduction moment in hamstring and patellar tendon anterior cruciate ligament reconstructed knees. Knee Surgery, Sport Traumatol Arthrosc. 2012;20(11):2214–2219. doi:10.1007/s00167-011-1835-z.

66. Westphal CJ, Schmitz A, Reeder SB, Thelen DG. Load-dependent variations in knee kinematics measured with dynamic MRI. J Biomech. 2013;46(12):2045–2052. doi:10.1016/j.jbiomech.2013.05.027. [PubMed: 23806309]

67. Whittington B, Silder A, Heiderscheit B, Thelen DG. The contribution of passive-elastic mechanisms to lower extremity joint kinetics during human walking. Gait Posture. 2008;27(4):628–634. doi:10.1016/j.gaitpost.2007.08.005. [PubMed: 17928228]

68. Zavras TD, Race A, Amis AA. The effect of femoral attachment location on anterior cruciate ligament reconstruction: Graft tension patterns and restoration of normal anterior-posterior laxity patterns. Knee Surgery, Sport Traumatol Arthrosc. 2005;13(2):92–100. doi:10.1007/s00167-004-0541-5.

69. Zavras TD, Race A, Bull AMJ, Amis AA. A comparative study of “isometric” points for anterior cruciate ligament graft attachment. Knee Surgery, Sport Traumatol Arthrosc. 2001;9(1):28–33. doi:10.1007/s001670000170.

What is known about the subject:

Abnormal tibiofemoral kinematics and cartilage loading patterns have previously been observed in ACL-reconstructed knees, with some evidence this may be associated with placement of the graft tunnels.

What this study adds to existing knowledge:

This study demonstrates that functional tibiofemoral kinematics, cartilage contact pressures, and ACL loading are sensitive to nonanatomic placement of the ACL graft.

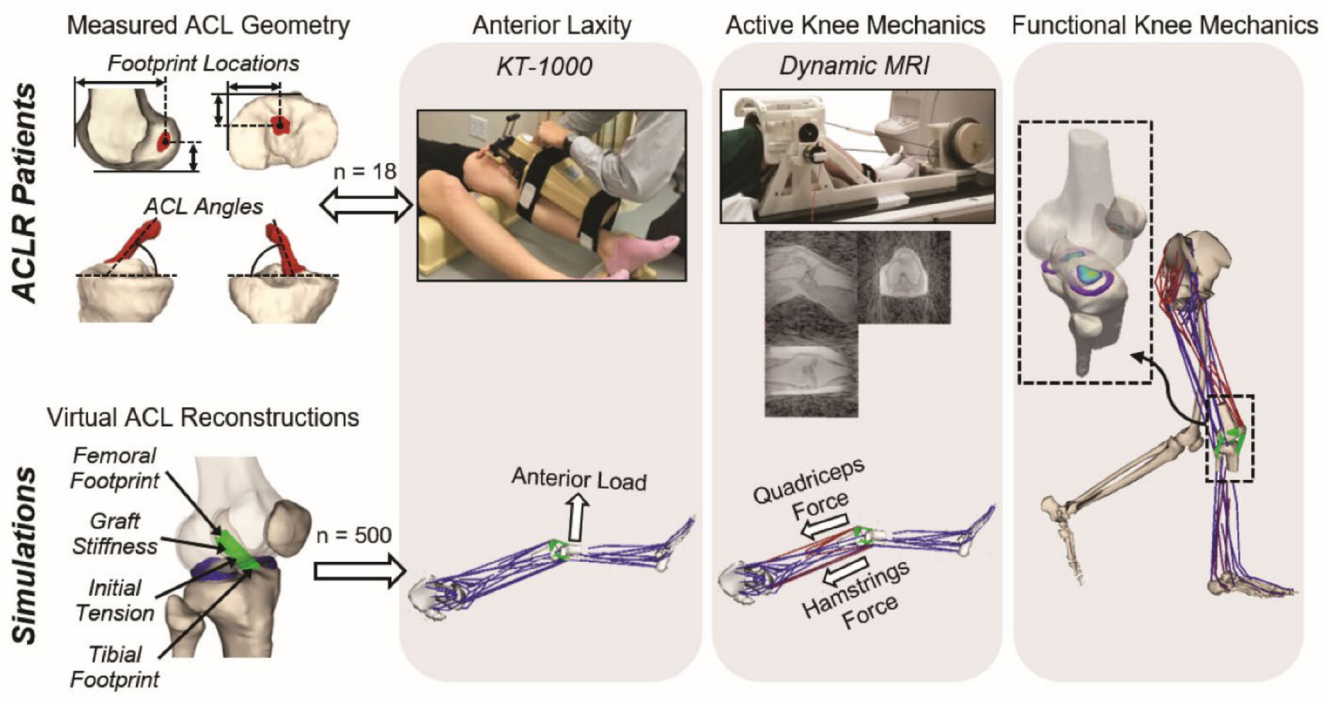

Figure 1:

Post-operative analysis of ACLR patients (top row) and virtual ACLR models (bottom row) were used to investigate the link between graft tunnel location and angles and knee mechanics. ACL geometries were reconstructed from MRIs to assess footprint locations and graft angle. Bilateral anterior knee laxity was evaluated at clearance from rehabilitation. Tibiofemoral kinematics during active knee motion were measured using dynamic MRI. For computational modeling, 500 virtual ACLR models were created by randomly varying the graft footprint locations, stiffness, and initial tension. An anterior knee laxity test, active knee extension, and walking were simulated for each virtual ACLR model.

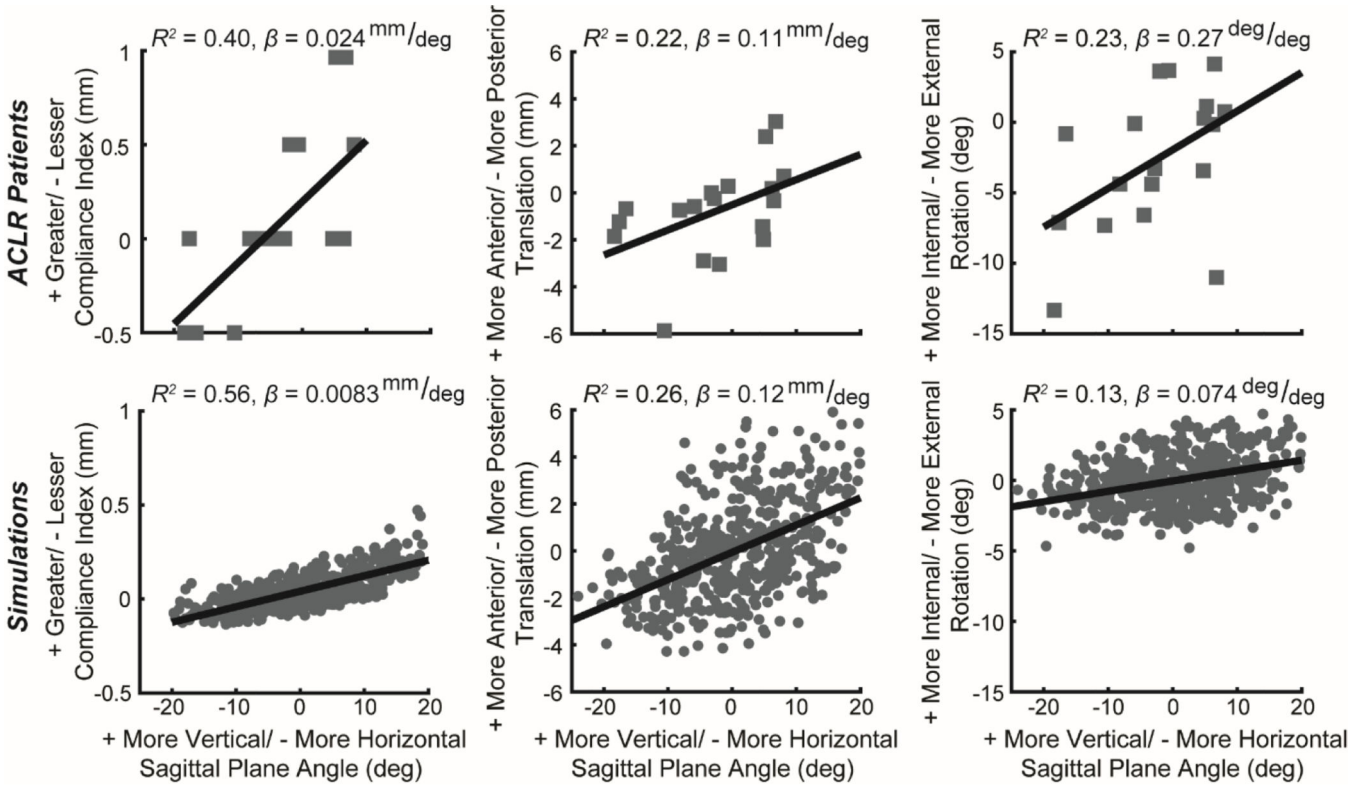

Figure 2:

Tibiofemoral kinematics exhibited similar relationship with sagittal plane graft angle in ACLR patients (top row) and ACLR simulations (bottom row). Specifically, a more vertical ACL graft was positively correlated with anterior knee laxity (compliance index) and both anterior tibial translation and internal tibial rotation during active knee extension (Table 1). For the ACLR patients, positive values indicate that the ACLR knee value was greater than that of the native knee, and negative values indicate that the ACLR knee value was less than that of the native knee. For the virtual ACLR model, positive values indicate that the model value was greater than that of the nominal model, and negative values indicate that the model value was less than that of the nominal model.

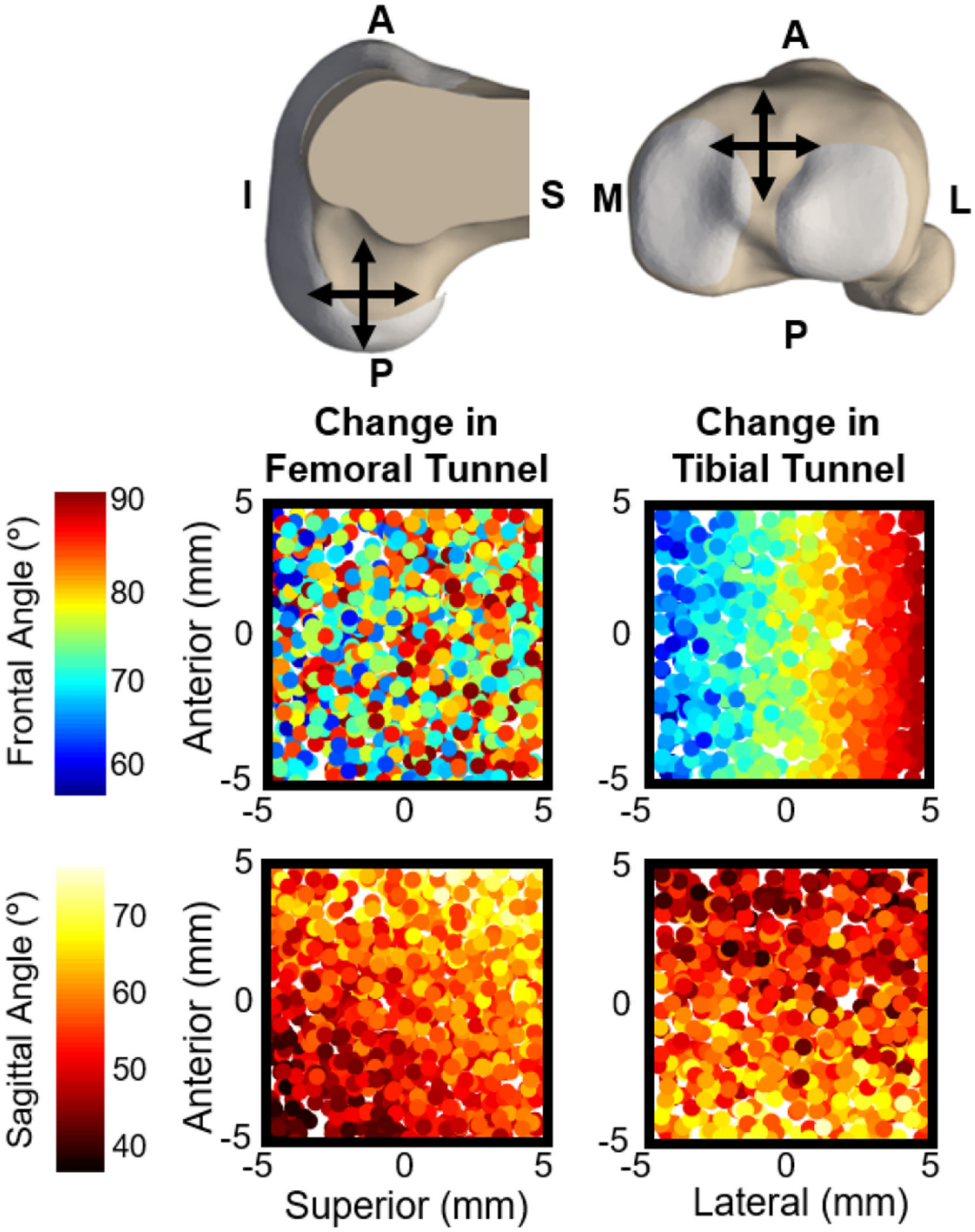

Figure 3:

Composite image shows how changes to the femoral (top-left) and tibial (top-right) tunnel locations alter the frontal and sagittal plane angles of the ACL graft. Each dot in the four scatter plots represents the tunnel location in one of the 500 virtual ACLR models. The color of each dot indicates the resulting ACL graft angles measured with the knee in full extension, given the femoral and tibial tunnel locations of that virtual ACLR model. From these scatter plots it is evident that femoral tunnel location does not systematically affect frontal plane angle of the graft. Femoral tunnel location does have a systematic effect on

sagittal plane angle of the graft with a more posterior-inferior femoral tunnel resulting in a less vertical graft in the sagittal plane and a more anterior-superior femoral tunnel resulting in a more vertical graft in the sagittal plane. Tibial tunnel location systematically affects both frontal and sagittal plane angle of the graft.

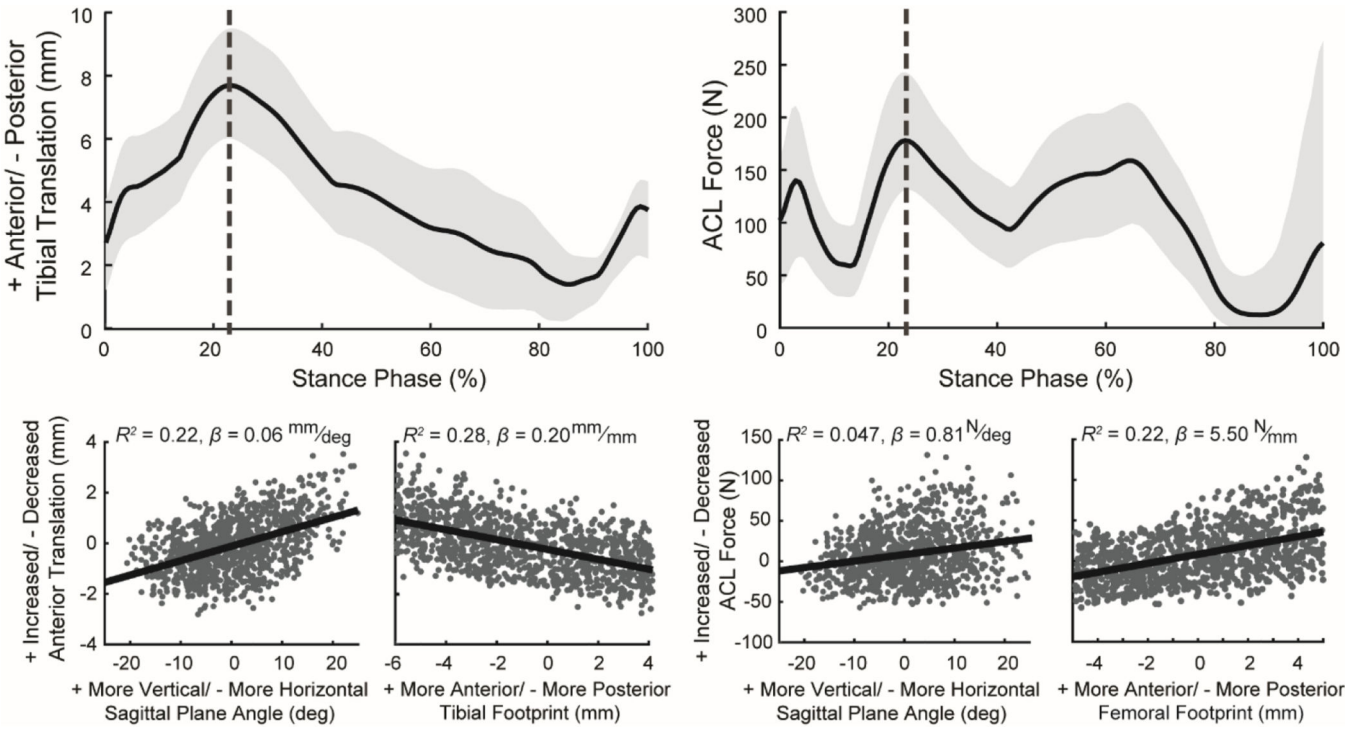

Figure 4:

Plots (top row) show the mean (black line) and the range between the 5th and 95th percentiles (light gray shaded region) for anterior tibial translation and ACL force during the stance phase of simulated walking for the 500 virtual ACL reconstructions (ACLR) with varying graft geometries, stiffnesses, and initial tensions. The scatter plots (bottom row) demonstrate the effect of changes in ACL graft tunnel locations and graft angle on anterior tibial translation and ACL force at the instance of peak ACL force during stance (vertical dotted gray line in top plots). Each point in the scatter plots was computed relative to the native model (virtual ACLR model minus native). Positive values indicate that the virtual ACLR model value was greater than that of the nominal model, and negative values indicate that the ACLR model value was less than that of the nominal model. Scatter plots include coefficient of determination (R^2) and the slope of the least-squares linear regression (β) computed between the ACL reconstruction surgical factors and the knee mechanics metrics.

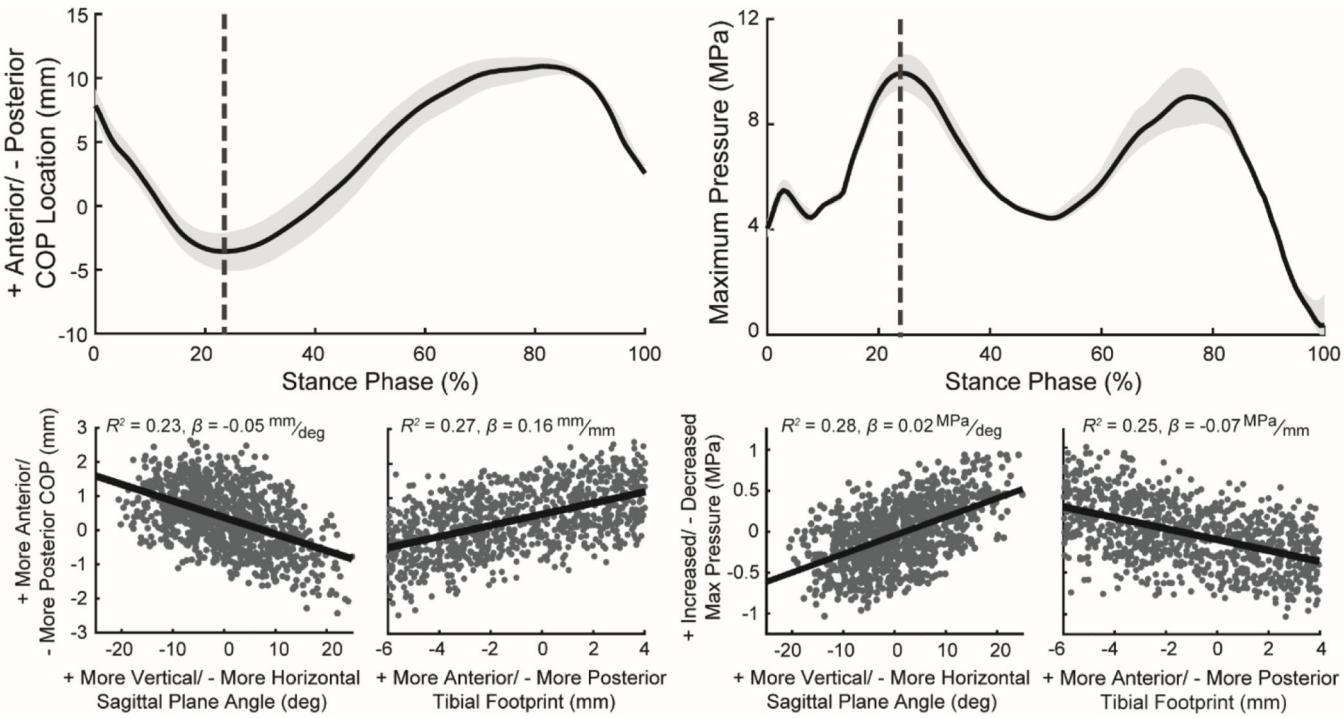

Figure 5:

Plots (top row) show the mean (line) and the range between the 5th and 95th percentiles (light gray shaded region) for the anterior center of pressure (COP) location and the maximum contact pressure on the medial tibial plateau during the stance phase of simulated walking for the 500 virtual ACL reconstructions (ACLR). The scatter plots (bottom row) demonstrate the effect of ACL graft tunnel location and graft angle on the anterior COP location and maximum contact pressure on the medial tibial plateau at the instance of peak ACL loading during stance (vertical dotted gray line in top plots). Each point in the scatter plots was computed relative to the native model (virtual ACLR model minus native). Positive values indicate that the virtual ACLR model value was greater than that of the nominal model, and negative values indicate that ACLR the model value was less than that of the nominal model. Scatter plots include coefficient of determination (R^2) and the slope of the least-squares linear regression (β) computed between the ACL reconstruction surgical factors and the knee mechanics metrics.

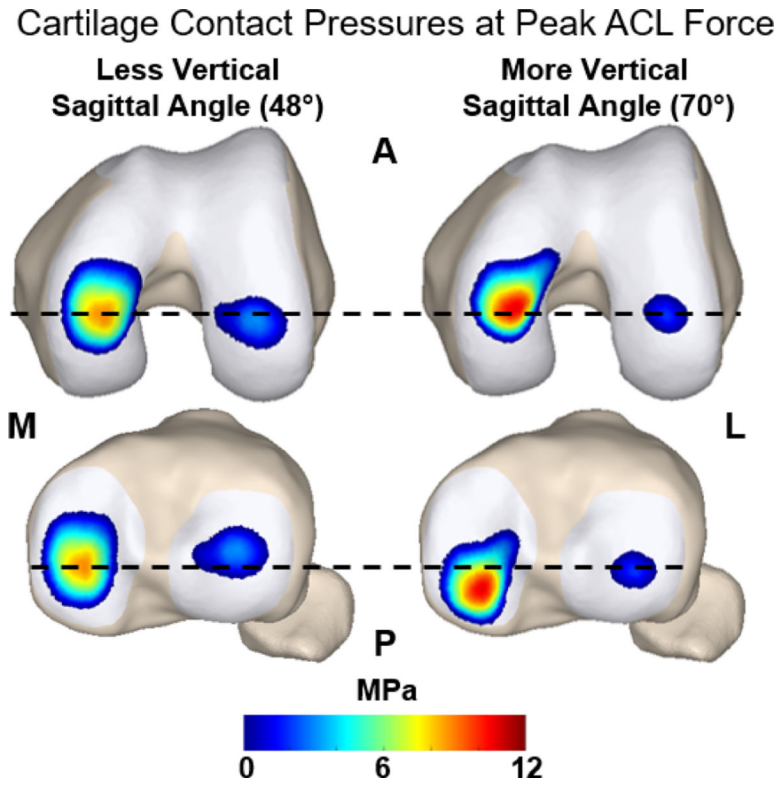

Figure 6:

Representative cartilage contact pressures at the instance of peak ACL force during simulated walking. A model with a less vertical sagittal graft angle (48°) is compared against a model with a more vertical sagittal graft angle (70°). The vertical graft resulted in larger anterior translation of the tibia relative to the femur. This manifested as the vertical graft leading to more anterior contact on the femur and more posterior contact on the tibial plateau. Additionally, a more vertical graft led to substantially greater contact pressure of the medial femoral and tibial cartilage surfaces.

Table 1:

Coefficient of determination (R^2) for significant ACLR patient ($P<0.05$) and corresponding computer simulation (Sim) linear regressions between non-anatomic ACL graft footprint location and angles and side-to-side differences in knee laxity, kinematics, and cartilage contact metrics.

		ACL Angle (deg)				Femoral Tunnel Location (mm)	
		Sagittal Plane		Frontal Plane		Superior	
		Patient R^2	Sim R^2	Patient R^2	Sim R^2	Patient R^2	Sim R^2
KT-1000 Measurement (mm)	Compliance Index	0.40	0.56	—	—	—	—
Tibiofemoral Rotations (deg)	Internal	0.23	0.13	—	—	—	—
	Adduction	0.44	0.14	—	—	—	—
Tibiofemoral Translations (mm)	Anterior	0.22	0.26	—	—	—	—
	Medial	—	—	0.23	0.74	0.29	0.25